

HyperEvent: Learning Cohesive Events for Large-scale Dynamic Link Prediction

Jian Gao, Jianshe Wu*, Jingyi Ding

Xidian University

Xi'an 710071 China

gaojian@xidian.edu.cn, jianshewu@126.com, jyding@xidian.edu.cn

Abstract

Dynamic link prediction in continuous-time dynamic graphs is a fundamental task for modeling evolving complex systems. Existing node-centric and event-centric methods focus on individual interactions or atomic states, failing to capture the structural cohesion of composite hyper-events—groups of causally related events. To address this, we propose HyperEvent, a framework reframing dynamic link prediction as hyper-event recognition. Central to HyperEvent is the dynamic construction of an association sequence using event correlation vectors. These vectors quantify pairwise dependencies between the query event and relevant historical events, thereby characterizing the structural cohesion of a potential hyper-event. The framework predicts the occurrence of the query event by evaluating whether it collectively forms a valid hyper-event with these historical events. Notably, HyperEvent outperforms state-of-the-art methods on 4 out of 5 datasets in the official leaderboard. For scalability, we further introduce an efficient parallel training algorithm that segments large event streams to enable concurrent training. Experiments validate HyperEvent’s superior accuracy and efficiency on large-scale graphs. Among which HyperEvent achieves a 6.95% improvement in Mean Reciprocal Rank over state-of-the-art baseline on the large-scale Flight dataset while utilizing only 10.17% of the training time.

Code — <https://github.com/jianjianGJ/HyperEvent>

Datasets —

https://tgb.complexdatalab.com/docs/leader_linkprop

1 Introduction

Temporal graphs model evolving systems through sequences of interactions (*i.e.*, temporal events), serving as essential abstractions for real-world dynamic systems like social networks and transaction networks (Min et al. 2021; Xu et al. 2025; Yan, Weihan, and Chang 2021). These graphs are primarily modeled as discrete-time graph snapshots or Continuous-Time Dynamic Graphs (CTDGs) (Liang et al. 2024). This work focuses specifically on CTDGs because real-world interactions intrinsically manifest as continuous streams of events, where preserving their exact temporal sequence is critical for capturing fine-grained event correlations. Accurately predicting future events within CTDGs,

known as dynamic link prediction, remains a core challenge with significant implications for applications such as real-time recommendation (Qin et al. 2024; Zhang et al. 2023), social networks (Daud et al. 2020; Dileo, Zignani, and Gaito 2024), traffic flow prediction (Zou et al. 2024; Ali et al. 2025), knowledge graphs (Ong et al. 2025; Chen et al. 2025), and anomaly detection (Duan et al. 2024; Yang, Zhao, and Shen 2025).

Recent advancements in CTDG representation learning demonstrate significant progress in dynamic link prediction. The evolution of CTDG representation learning has bifurcated into two dominant paradigms: node-centric and event-centric approaches.

Node-centric methods primarily model temporal dynamics through evolving node embeddings. They track node states via RNNs and graph convolutions (Rossi et al. 2020; Kumar, Zhang, and Leskovec 2019; Rakshit Trivedi and Zha 2019; Zhang et al. 2024). While scalable and inductive, these methods often reduce events to pairwise node embeddings, potentially overlooking complex inter-event relationships. Event-centric approaches explicitly model events as first-class entities. Such as CAWN anonymizes temporal motifs via causal walks to capture structural patterns (Wang et al. 2021b). GraphMixer and DyGFormer further reveal that lightweight architectures (*e.g.*, patched Transformers, time-aware MLPs) can effectively encode event sequences without complex RNNs or graph convolutions (Cong et al. 2023; Yu et al. 2023). However, event-centric methods focus on customized embeddings for stacked events and lack explicit mechanisms to model the structural cohesion between events.

Current paradigms overlook a crucial aspect of complex temporal events: the cohesive structure of composite events. Sequences of individual events often have intrinsic causal or synergistic relationships forming larger, meaningful hyper-events. For instance in figure 1, sequential transactions like a credit card purchase at a taxi service (t_1), followed by food (t_2), grocery (t_3), cinema (t_4), and drink (t_5) — despite occurring at distinct timestamps — collectively form a cohesive “shopping trip” hyper-event in transaction networks. Existing methods fail to explicitly model these vital event correlations. They treat dynamic link prediction as a function of aggregated but atomized node or node-pair states instead of recognizing the holistic signature of a unified com-

*Corresponding author.

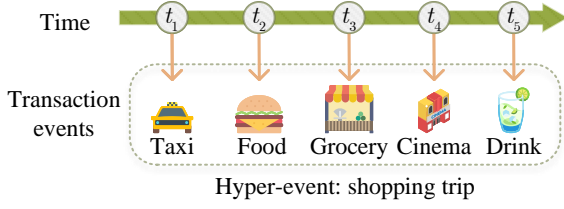


Figure 1: A hyper-event comprising five events.

posite hyper-event.

Moreover, many methods struggle with scalability issues when processing large scale event streams. While node-centric methods often use a memory-based architecture to store the node embeddings, which require sequential state updates per event, limiting training efficiency and parallelization. Approaches delving deeper into complex event contexts or mutual neighborhood modeling incur even higher computational costs. Consequently, scaling to real-world, large-scale temporal graphs remains a significant challenge.

To overcome these limitations, we propose HyperEvent, an novel framework for dynamic link prediction in CT-DGs. HyperEvent fundamentally shifts the predictive task: instead of predicting individual links based solely on node states, it identifies complete hyper-events. A hyper-event is a cohesive set of temporally related events. The core insight is that a query link is likely to occur if and only if it completes a valid hyper-event when combined with relevant historical events. HyperEvent achieves this by introducing an event correlation vector to capture pairwise associations between events. It dynamically constructs a relation sequence characterizing the entire hyper-event without complex parameter learning. This event-level focus naturally captures intrinsic temporal dependencies and boosts prediction accuracy. Furthermore, we develop a highly scalable training algorithm. Leveraging precomputed adjacency tables and segmenting large event streams into parallelizable segments, HyperEvent efficiently trains on real-world, large-scale datasets. This work presents the following contributions:

1) The HyperEvent Framework: HyperEvent presents a novel framework that reframes CTDGs learning for dynamic link prediction, shifting focus from predicting isolated edges to recognizing composite higher-order events.

2) Modeling Event Correlations: HyperEvent introduces an efficiently computed association sequence capturing relational patterns between historical events and the query event. This provides richer contextual information than node-centric or event-centric methods.

3) Scalable Training Algorithm: HyperEvent incorporates an efficient parallel training algorithm, significantly enhancing training efficiency and scalability for large graphs.

4) Empirical Validation: Extensive experiments on multiple benchmark datasets demonstrate HyperEvent’s competitive prediction accuracy and the effectiveness of its parallel training on large-scale graphs.

2 Related Works

Temporal Graph Learning. Research on temporal graph learning has evolved from discrete snapshot aggregation to methods directly processing event streams. Discrete-time techniques partition edge streams into fixed-interval snapshots (Pareja et al. 2020; Manessi, Rozza, and Manzo 2020; Goyal, Chhetri, and Canedo 2020; Hajiramezanali et al. 2019), applying Graph Neural Networks (Scarselli et al. 2008; Kipf and Welling 2017) and temporal models like RNNs (Hochreiter and Schmidhuber 1997; Cho et al. 2014) or Transformers (Vaswani et al. 2017) separately to each snapshot. However, these methods inherently suffer from information loss due to predetermined aggregation granularity, motivating direct processing of continuous event streams.

Node-Centric Continuous-Time Models. Pioneering continuous-time approaches leverage recurrent architectures to maintain node memories. JODIE uses coupled RNNs for mutual user-item updates (Kumar, Zhang, and Leskovec 2019), while DyRep incorporates multi-hop dynamics at increased complexity (Rakshit Trivedi and Zha 2019). The Temporal Graph Network (TGN) framework unifies memory modules with graph propagation (Rossi et al. 2020), adopted by TGAT for temporal attention-based neighbor aggregation (Xu et al. 2020). Despite scalability improvements, these methods remain fundamentally node-centric – sequentially updating node states through event-by-event processing creates computational bottlenecks and constrains parallelization. Recent innovations like TNCN accelerate training via asynchronous propagation (Zhang et al. 2024), and EDGE employs graph partitioning (Chen et al. 2021), yet they retain the core limitation of ignoring holistic event semantics.

Event-Centric Continuous-Time Models. Beyond node embeddings, recent approaches explicitly model event interactions. CAWN encodes causal anonymous walks to capture temporal motifs but incurs prohibitive sampling costs (Wang et al. 2021b). NAT constructs reusable neighbor caches (Luo and Li 2022), while DyGFormer applies Transformers to patched neighbor co-occurrences (Yu et al. 2023). Though these improve topological awareness, they fail to model intrinsic correlations between constituent events within higher-order structures. TCL constructs temporal dependency graphs but inherits RNN limitations for long-range dependencies (Wang et al. 2021a). Continuous-time neural ODE approaches like CTAN enable non-dissipative propagation yet overlook event-level dynamics (Gravina et al. 2024).

3 Method

3.1 Preliminaries and Problem Formulation

Continuous-time Dynamic Graph: A continuous-time dynamic graph represents the dynamics of interactions between entities over a continuous timeline. Formally, it is as a chronologically ordered sequence of interaction events: $\mathcal{G} = \{(u_1, v_1, t_1), (u_2, v_2, t_2), \dots, (u_n, v_n, t_n)\}$, where $t_1 \leq t_2 \leq \dots \leq t_n$. Each event (u_i, v_i, t_i) signifies an interaction occurring at timestamp t_i between a source node

u_i and a destination node v_i , both belonging to the universal node set \mathcal{V} .

Dynamic Link Prediction: The dynamic link prediction task aims to forecast future interactions based on the observed historical evolution of the graph. Given the sequence of all events occurring strictly before a query time t^* , denoted as $\mathcal{E}_{<t^*} = \{(u, v, t) \in \mathcal{G} \mid t < t^*\}$, the task is to predict the existence of a specific interaction between nodes u^* and v^* at time t^* . Formally, the goal is to determine the likelihood $P((u^*, v^*, t^*) \text{ occurs} \mid \mathcal{E}_{<t^*})$.

3.2 Existing Frameworks

Node-centric methods Node-centric methods jointly leverage spatial and temporal models to construct dynamic node embeddings. The framework operates as follows:

$$\mathbf{h}_u(t) = \Psi_{\text{temp}}(\mathbf{h}_u(t^-), \Psi_{\text{spatial}}(\{\mathbf{h}_v(t^-) \mid v \in \mathcal{N}_u(t)\})) \quad (1)$$

where Ψ_{spatial} aggregates topological information from neighboring nodes $\mathcal{N}_u(t)$ (e.g., via GNNs), Ψ_{temp} updates the state using sequential models (e.g., RNNs), and t^- denotes the timestamp immediately before t . For link prediction at t^* , the likelihood is computed as:

$$P((u^*, v^*, t^*) \in \mathcal{E}) = \sigma(\mathbf{W}^\top [\mathbf{h}_{u^*}(t^{*-}) \oplus \mathbf{h}_{v^*}(t^{*-})] + b) \quad (2)$$

where σ is the sigmoid function, \mathbf{W} and b are learnable parameters of a linear scoring unit, \oplus denotes concatenation.

In practical implementations, the update frequency in equation (1) significantly influences training efficiency, leading to the common approach of updating at intervals of Δt as a compromise.

Limitations: This framework faces fundamental constraints preventing parallelization: 1) *Causality Lock*: Embedding $\mathbf{h}_u(t)$ depends strictly on all prior events involving u . This sequential dependency forces event-by-event training. 2) *Temporal Resolution Dilemma*: Ideal granularity ($\Delta t = 1$) requires updating node embeddings after every event, maximally preserving recent context but incurring prohibitive $|\mathcal{E}|$ sequential steps for per-epoch training. Practical minibatching sets $\Delta t = \text{batch duration}$, updating embeddings only at batch boundaries. This skips events within the batch interval $[t^* - \Delta t, t^*)$, discarding critical short-term dependencies. Using outdated embeddings $\mathbf{h}(t^* - \Delta t)$ to score links at t^* ignores crucial events near t^* when $\Delta t > 1$. This significantly degrades accuracy on high-activity graphs.

Event-centric Methods For a query event $e^* = (u^*, v^*, t^*)$, these methods first identify a relevant event sub-set \mathcal{S}_{e^*} via neighborhood sampling:

$$\mathcal{S}_{e^*} = \{e_k \mid \phi(u^*, v^*, u_k, v_k, |t^* - t_k|) \leq \delta, t_k < t^*\}, \quad (3)$$

where $\phi(\cdot)$ is a heuristic proximity function (e.g., temporal or structural closeness) and δ a threshold.

The event feature matrix $\mathbf{M}_{e^*} \in \mathbb{R}^{|\mathcal{S}_{e^*}| \times d}$ is constructed by aggregating features:

$$\mathbf{M}_{e^*} = \begin{bmatrix} \mathbf{x}_1 \\ \vdots \\ \mathbf{x}_{|\mathcal{S}_{e^*}|} \end{bmatrix}, \quad \forall e_i \in \mathcal{S}_{e^*}. \quad (4)$$

Here, \mathbf{x} denotes customized event features, which can be constructed by concatenating edge features and node features, or incorporating other tailored features (such as co-neighbor encoding), along with temporal encoding.

A sequence encoder (e.g., Transformer) processes \mathbf{M}_{e^*} to produce the query's predictive representation:

$$\mathbf{h}_{e^*} = \text{Encoder}(\mathbf{M}_{e^*}). \quad (5)$$

The existence probability of e^* is computed as:

$$P((u^*, v^*, t^*) \in \mathcal{E}) = \sigma(\mathbf{w}^\top \mathbf{h}_{e^*} + b), \quad (6)$$

where \mathbf{w} and b are learnable parameters, and $\sigma(\cdot)$ is the sigmoid function.

Limitations: This framework suffers from four critical weaknesses: 1) *Feature Dependency*: Performance heavily relies on pre-existing node/edge features. When features are absent—common in real-world event streams—manual initialization (e.g., zero vectors) creates informationless inputs, degrading model reliability. 2) *Atomic Aggregation*: The stacking operation \mathbf{M}_{e^*} treats events as isolated entities, disregarding latent inter-event correlations within \mathcal{S}_{e^*} that could elucidate complex interaction dynamics. 3) *Relational Blindness*: By operating solely on raw features, the approach fails to explicitly model structural or temporal dependencies between events, leading to suboptimal context representation. 4) *Computational Overhead*: The $\phi(\cdot)$ -based sampling requires expensive neighborhood searches for every query, incurring $O(|\mathcal{E}|)$ complexity that prohibits scalability to large-scale graphs.

3.3 HyperEvent Framework

HyperEvent fundamentally redefines dynamic link prediction as the verification of hyper-event. Instead of learning stacked isolated event embeddings, it predicts whether a query event $e^* = (u^*, v^*, t^*)$ forms a consistent *hyper-event* \mathcal{H}_{e^*} with relevant historical events. A hyper-event represents an integrated interaction pattern where constituent events exhibit intrinsic relational dependencies. The existence probability of e^* is derived from the authenticity of \mathcal{H}_{e^*} :

$$P((u^*, v^*, t^*) \in \mathcal{E}) = D(\mathcal{H}_{e^*}) \quad (7)$$

where $D(\cdot) \in \{0, 1\}$ is the hyper-event discriminator.

Figure 2 presents the methodological framework of the HyperEvent. The framework consists of four steps: 1) Real-time Adjacency Table Maintenance; 2) Hyper-Event Extraction; 3) Pairwise Correlation Encoding; 4) Authenticity Discrimination. Subsequent sections detail the design of each component.

Real-time Adjacency Table Maintenance (① in Figure 2)

Inspired by the embedding updates in node-centric methods (Section 3.2), HyperEvent maintains a dynamic adjacency table \mathcal{A} . For each node $v \in \mathcal{V}$, \mathcal{A}_v stores the n_{neighbor} most recent interaction partners ordered chronologically:

$$\mathcal{A}_v(t) = [(v_1, \tau_1), \dots, (v_k, \tau_k)], \quad (8)$$

where $t > \tau_1 > \tau_2 > \dots > \tau_k$ and $k \leq n_{\text{neighbor}}$. Here, n_{neighbor} controls the storage overhead of the adjacency table

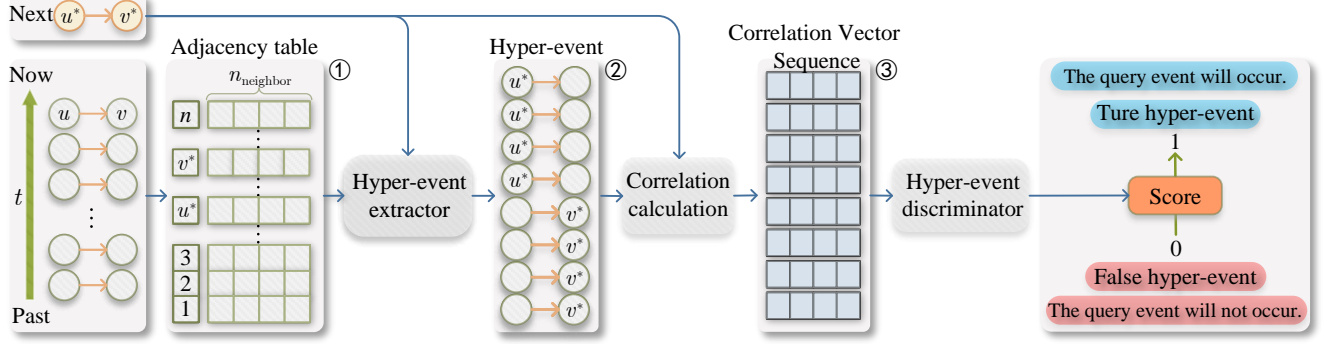


Figure 2: The HyperEvent framework.

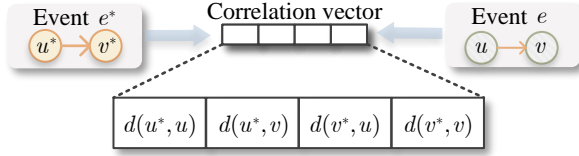


Figure 3: Event correlation vector.

and critically defines the historical depth considered when constructing hyper-events for a node, enabling efficient aggregation of relevant events. Specifically, a smaller n_{neighbor} value prioritizes short-term historical interactions, enhancing sensitivity to immediate dynamics, whereas a larger value incorporates long-term contextual patterns, capturing enduring relationships. Practical event prediction scenarios exhibit distinct preferences: for instance, in highly dynamic environments like social networks where interactions evolve rapidly, a lower n_{neighbor} (e.g., near 10) is preferable to adapt swiftly to recent changes; conversely, in stable relational settings such as collaboration networks, a higher n_{neighbor} (e.g., near 50) better utilizes extensive historical data to improve accuracy. Empirical results shows that $n_{\text{neighbor}}=10-50$ suffices for most datasets, balancing computational efficiency and contextual richness.

All variables in the method are computed in real time, the time term t is omitted in subsequent descriptions for conciseness.

Hyper-event Extraction (② in Figure 2) For query event $e^* = (u^*, v^*, t^*)$, extract n_{latest} relevant events for both u^* and v^* directly from \mathcal{A} :

$$\mathcal{S}_{u^*} = \text{Top-}n_{\text{latest}} \text{ events from } \mathcal{A}_{u^*}, \quad (9)$$

$$\mathcal{S}_{v^*} = \text{Top-}n_{\text{latest}} \text{ events from } \mathcal{A}_{v^*}. \quad (10)$$

The hyper-event candidate \mathcal{H}_{e^*} is constructed as:

$$\mathcal{H}_{e^*} = \mathcal{S}_{u^*} \cup \mathcal{S}_{v^*}. \quad (11)$$

Pairwise Correlation Encoding (③ in Figure 2) As shown in figure 3, for each event $e = (u, v, t) \in \mathcal{H}_{e^*}$, compute a four-dimensional *relational vector* \mathbf{r} capturing its

structural-temporal correlations with e^* :

$$\mathbf{r} = [d(u^*, u), d(u^*, v), d(v^*, u), d(v^*, v)]^\top. \quad (12)$$

$d(a, b)$ is a distance metric that measures the overlap of 1-hop temporal neighborhoods between two nodes.

$$d(a, b) = \frac{1}{|\mathcal{A}_a| \cdot |\mathcal{A}_b|} \sum_{i=1}^{|\mathcal{A}_a|} \sum_{j=1}^{|\mathcal{A}_b|} \mathbb{I}[\mathcal{A}_a(i) = \mathcal{A}_b(j)], \quad (13)$$

where \mathbb{I} is the indicator function. This yields a 4-dimensional relational feature sequence $\mathbf{R}_{\mathcal{H}_{e^*}} = [\mathbf{r}_1, \mathbf{r}_2, \dots, \mathbf{r}_{|\mathcal{H}_{e^*}|}]$.

Enhanced Correlation Vector Sequence: To comprehensively capture the higher-order correlations, we further propose 0-hop and 2-hop correlation.

i) *0-hop correlation:* Measures the direct co-occurrence frequency between nodes by computing the proportion of a node's temporal neighbors that equal the target node. Formally:

$$d^{(0)}(a, b) = \frac{1}{|\mathcal{A}_b|} \sum_{j=1}^{|\mathcal{A}_b|} \mathbb{I}[a = \mathcal{A}_b(j)]. \quad (14)$$

This quantifies asymmetric dependence, where $d^{(0)}(a, b)$ reflects the likelihood of a appearing in b 's direct historical interactions.

ii) *2-hop correlation:* Evaluates 2-hop neighborhood similarities while maintaining computational tractability. The neighborhood expansion is constrained to top $\lfloor \sqrt{n_{\text{neighbor}}} \rfloor$ neighbors $\tilde{\mathcal{A}}_a$, then compute:

$$d^{(2)}(a, b) = \frac{1}{|\tilde{\mathcal{A}}_a^{(2)}| \cdot |\tilde{\mathcal{A}}_b^{(2)}|} \sum_{i=1}^{|\tilde{\mathcal{A}}_a^{(2)}|} \sum_{j=1}^{|\tilde{\mathcal{A}}_b^{(2)}|} \mathbb{I}[\tilde{\mathcal{A}}_a^{(2)}(i) = \tilde{\mathcal{A}}_b^{(2)}(j)], \quad (15)$$

with $\tilde{\mathcal{A}}_a^{(2)} = \bigcup_{x \in \tilde{\mathcal{A}}_a} \tilde{\mathcal{A}}_x$. $\tilde{\mathcal{A}}$ means top- $\lfloor \sqrt{n_{\text{neighbor}}} \rfloor$ part of \mathcal{A} . The $\sqrt{\cdot}$ ensures computational complexity aligns with the 1-hop metric.

The integrated relational vector concatenates correlations

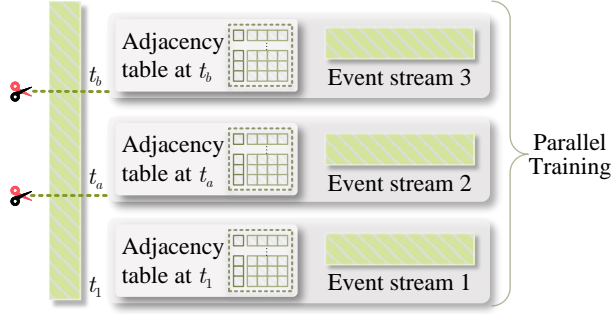


Figure 4: Parallelized training framework. Adjacency tables precomputed at key timestamps (t_1, t_2, t_3).

for all node pairs between e and e^* :

$$\mathbf{r} = [d^{(0)}(u^*, u), d^{(0)}(u^*, v), d^{(0)}(v^*, u), d^{(0)}(v^*, v), \\ d(u^*, u), d(u^*, v), d(v^*, u), d(v^*, v), \\ d^{(2)}(u^*, u), d^{(2)}(u^*, v), d^{(2)}(v^*, u), d^{(2)}(v^*, v)] \quad (16)$$

This 12-dimensional representation holistically encodes multi-scale structural dependencies within the hyper-event candidate. The relational sequence $\mathbf{R}_{\mathcal{H}_{e^*}} = [\mathbf{r}_1, \mathbf{r}_2, \dots, \mathbf{r}_{|\mathcal{H}_{e^*}|}]$ preserves chronological order of events in \mathcal{H}_{e^*} , enabling downstream models to exploit temporal dynamics while mitigating information loss in higher-order neighborhood abstraction.

Although the complexity of Equations (13) and (15) is $O(n_{\text{neighbor}}^2)$, this remains efficient due to GPU-accelerated tensor parallelism and the small, empirically configured neighborhood size $n_{\text{neighbor}} \in [10, 50]$.

Hyper-event Discriminator Finally, an Transformer-based encoder is used as the hyper-event discriminator, which processes $\mathbf{R}_{\mathcal{H}_{e^*}}$ to classify \mathcal{H}_{e^*} 's authenticity:

$$D(\mathcal{H}_{e^*}) = \sigma(\mathbf{w}^\top \text{Transformer}(\mathbf{R}_{\mathcal{H}_{e^*}}) + b), \quad (17)$$

where σ denotes the sigmoid function. Binary cross-entropy loss is employed to optimize the discriminator:

$$\mathcal{L} = - \sum_{\mathcal{H}_{e^*}} \left[y \log D(\mathcal{H}_{e^*}) + (1 - y) \log (1 - D(\mathcal{H}_{e^*})) \right] \quad (18)$$

where $y = 1$ if the query event e^* represents a true interaction, and $y = 0$ otherwise.

Advantages over Event-centric Methods: 1). *Feature Agnosticism*: Eliminates dependency on pre-defined features by deriving relational vectors purely from interaction history. 2). *Holistic Pattern Modeling*: Explicitly encodes inter-event dependencies within \mathcal{H}_{e^*} via \mathbf{r}_k , overcoming atomic aggregation. 3). *Relational Inductivity*: Temporal cross-distance $d(\cdot, \cdot)$ intrinsically models structural-temporal relationships. 4). *Constant-Time Extraction*: $\mathcal{O}(1)$ hyper-event retrieval via \mathcal{A} replaces $\mathcal{O}(|\mathcal{E}|)$ neighborhood sampling. 5). *Scalability*: Enables graph segmentation and parallel training through pre-calculated adjacency tables.

3.4 Efficient Training Algorithm

The HyperEvent architecture fundamentally differs from existing methods through its dependence on adjacency tables rather than learned node states. This enables segmentation-based training: given an adjacency table at any starting timestamp, HyperEvent can commence training from that precise temporal point without loss of continuity. Consequently, precomputed adjacency tables are only required at segment boundaries, which are efficiently obtainable through cumulative aggregation.

Finally, the event streams in each segment can be trained in parallel. As illustrated in Figure 4, the proposed method partitions the original event stream \mathcal{G} into multiple non-overlapping segments. Each segment corresponds to a distinct time interval demarcated by split points. Crucially, adjacency tables are precomputed at the starting timestamp of every segment, capturing the cumulative graph state up to that point. This precomputation mechanism, detailed in Section 3.3, ensures that the cumulative structural information captured at segmentation boundaries is functionally equivalent to that obtained during continuous sequential processing.

Efficient Implementation. HyperEvent achieves exceptional computational efficiency, which ensures scalability and real-time applicability in large-scale temporal graphs. The exhaustive complexity analyses are elaborated in the supplementary material. Furthermore, the parallel training paradigm fundamentally leverages tensorization rather than conventional multi-threading implementation. Crucially, all computations within the framework operate directly on tensors, inherently enabling batched parallel execution on GPUs. Specifically, the original event stream tensor, shaped as $(|\mathcal{E}|, 2)$, is partitioned into segments, transforming it into a $(n_{\text{segment}}, \lceil |\mathcal{E}|/n_{\text{segment}} \rceil, 2)$ tensor, where padding with a designated value (-1) is applied to handle event counts not perfectly divisible by the segment count. Computational operations defined for HyperEvent naturally extend by introducing an additional segment dimension. This tensor-centric parallelism bypasses the computational overhead intrinsic to CPU multi-threading and eliminates constraints imposed by finite CPU core counts.

4 Experiment

4.1 Experimental Setup

HyperEvent is evaluated using the Temporal Graph Benchmark (TGB) (Huang et al. 2023), adhering to its standardized evaluation protocols with filtered Mean Reciprocal Rank (MRR) as the metric. TGB provides five benchmark datasets for dynamic link prediction: tgbl-wiki-v2 (Wiki), tgbl-review-v2 (Review), tgbl-coin-v2 (Coin), tgbl-comment (Comment), and tgbl-flight-v2 (Flight). Notably, Comment (44 million events) and Flight (67 million events) represent large-scale graphs. Optimal hyperparameters were determined via grid search. As the Transformer architecture within HyperEvent is not a contribution of this work, a fixed configuration was employed. Further details regarding datasets, evaluation metrics, specific hyperparameters,

Model	Wiki	Review	Coin	Comment	Flight
EdgeBank _∞	49.5	2.3	45.2	12.9	16.7
EdgeBank _{tw}	57.1	2.5	35.9	14.9	38.7
JODIE	63.1±1.7	34.7±0.1	OOM	OOM	OOM
DyRep	5.0±1.7	22.0±3.0	45.2±4.6	28.9±3.3	55.6±1.4
TGAT	14.1±0.7	35.5±1.2	OOM	OOM	OOM
TGN	39.6±6.0	34.9±2.0	58.6±3.7	37.9±2.1	70.5±2.0
CAWN	71.1±0.6	19.3±0.1	OOM	OOM	OOM
NAT	74.9±1.0	34.1±2.0	OOM	OOM	OOM
TCL	20.7±2.5	19.3±0.9	OOM	OOM	OOM
GraphMixer	11.8±0.2	52.1±1.5	OOM	OOM	OOM
DyGFormer	79.8±0.4	22.4±1.5	75.2±0.4	67.0±0.1	OOM
TNCN	71.8±0.4	37.7±1.0	76.2±0.4	69.7±0.6	82.0±0.4
CTAN	66.8±0.7	40.5±0.4	74.8±0.4	67.1±6.7	OOM
HyperEvent	80.9±0.1	26.8±0.4	77.3±0.3	75.9±0.2	87.7±0.3

Table 1: MRR of methods on different datasets. The best-performing method on each dataset is highlighted in bold-face, while the second-best is indicated with an underline. ‘OOM’ denotes out-of-memory errors.

training, and experimental hardware are provided in the supplementary material. For clarity in tables and figures, all reported MRR values are presented as percentages (i.e., scaled by 100).

4.2 Baselines

HyperEvent is compared against the following temporal graph representation learning and dynamic link prediction methods, as introduced in Related Works:

Non-parametric methods: EdgeBank_∞, EdgeBank_{tw} (Pour-safaei et al. 2022).

Deep learning methods: JODIE (Kumar, Zhang, and Leskovec 2019), DyRep (Rakshit Trivedi and Zha 2019), TGAT (Xu et al. 2020), TGN (Rossi et al. 2020), CAWN (Wang et al. 2021b), NAT (Luo and Li 2022), TCL (Wang et al. 2021a), GraphMixer (Cong et al. 2023), DyGFormer (Yu et al. 2023), TNCN (Zhang et al. 2024), CTAN (Gravina et al. 2024).

4.3 Baseline Comparison

Table 1 presents the MRR of HyperEvent against 12 state-of-the-art baselines. HyperEvent achieves state-of-the-art performance on four datasets: Wiki (80.9), Coin (77.3), Comment (75.9), and Flight (87.7). Crucially, it surpasses the current top methods on the TGB leaderboard by significant margins¹, improving MRR by 1.1% (vs. DyGFormer) on Wiki, 1.1% (vs. TNCN) on Coin, 6.2% (vs. TNCN) on Comment, and 5.7% (vs. TNCN) on Flight. These gains validate HyperEvent’s core innovation: modeling interdependencies among correlated events within a hyper-event significantly enhances dynamic link prediction. HyperEvent uniquely captures holistic structural-temporal patterns that node-centric or isolated-event embeddings fail to represent, particularly in high-churn networks with complex event clusters.

¹https://tgb.complexdatalab.com/docs/leader_linkprop/

Method	Metric		
	Training Time per Epoch	GPU Memory	MRR
TNCN(SOTA)	10h 34m 37s	15,189MB	82.0
HyperEvent(ours)	1h 4m 33s	2,346MB	87.7
Improvement	89.83% ↓	84.55% ↓	6.95% ↑

Table 2: Efficiency of HyperEvent on Flight dataset.

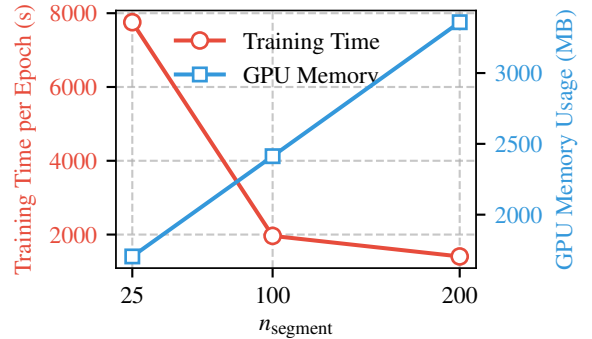


Figure 5: GPU memory usage and per-epoch training duration of HyperEvent across varying segment counts (n_{segment}).

However, on the Review dataset, HyperEvent achieves an MRR of 26.8, underperforming methods like GraphMixer (52.1) and CTAN (40.5). This phenomenon can be attributed to two dataset-specific factors:

- 1) *High Temporal Surprise:* With a surprise metric of 0.987 (the highest among datasets), Review exhibits highly unpredictable interactions. HyperEvent’s reliance on historical event correlations becomes less effective when future events deviate substantially from past structures.
- 2) *Sparse Event Context:* Predicting “which product a user reviews next” relies heavily on individual user behavior rather than inter-event dependencies. This misalignment with HyperEvent’s strength in modeling group dynamics reduces its relative advantage.

The exceptional performance on Coin, Comment, and Flight—datasets featuring dense event streams, and strong temporal dependencies reinforces HyperEvent’s superiority in scenarios where event interdependencies drive evolutionary patterns. HyperEvent establishes a new paradigm for temporal graph representation learning, particularly in applications demanding holistic event-sequence reasoning.

4.4 Effectiveness of the Training Algorithm

The efficiency gains of HyperEvent are quantified in Table 2, contrasting HyperEvent with TNCN – the current SOTA approach topping the TGB Flight dataset leaderboards. HyperEvent achieves a remarkable 89.83% reduction in per-epoch training time (1h 4m 33s vs. TNCN’s 10h 34m 37s) and an 84.55% reduction in GPU memory consumption (2,346MB vs. 15,189MB), while simultaneously improving prediction

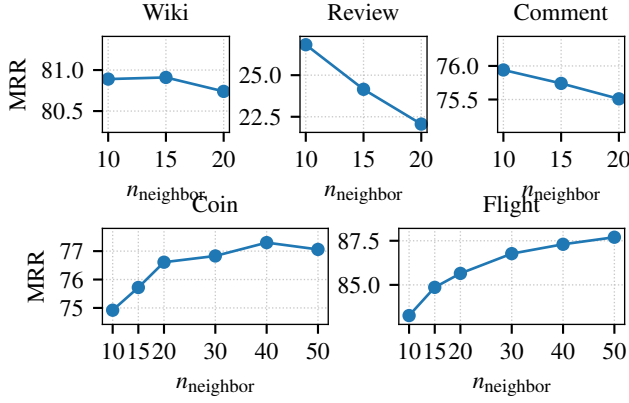


Figure 6: MRR across different datasets under varying $n_{neighbor}$ (fix $n_{latest} = 10$).

accuracy with a 6.95% higher MRR (87.7 vs. 82.0). These results unequivocally validate the efficacy of HyperEvent’s training algorithm. The efficiency stems from three key innovations: First, segmenting the event stream into parallelizable segmentations reduces the iterations per epoch by a factor of $n_{segment}$. Second, a tensorized implementation leverages GPU parallelism directly, bypassing multi-threading bottlenecks and CPU-GPU communication latency. Third, the low-dimensional design of the event correlation vectors (only 12 dimensions) and the lightweight classification model significantly reduce the memory footprint.

Further analysis of computational trade-offs is illustrated in figure 5, which plots GPU memory usage and per-epoch training duration against varying segment counts ($n_{segment}$). The segment count critically balances memory efficiency and training speed: increasing $n_{segment}$ linearly escalates memory demands (blue curve), as $n_{segment}$ adjacency tables must be stored concurrently. Conversely, training time initially decreases nearly linearly (red curve, $n_{segment} < 100$) due to heightened parallelism. Beyond this threshold, diminishing returns emerge as GPU computational bottlenecks saturate; further increasing $n_{segment}$ yields marginal speed improvements despite continued memory growth. This underscores the algorithm’s adaptability, where $n_{segment}$ can be tuned to align with hardware constraints.

Collectively, these results demonstrate HyperEvent’s dual breakthrough: it establishes a new SOTA in prediction accuracy while revolutionizing computational efficiency.

4.5 Modulating Long- and Short-Term Preferences via $n_{neighbor}$

The influence of historical context depth on dynamic link prediction performance is investigated by analyzing the impact of varying the hyperparameter $n_{neighbor}$ across diverse datasets. As shown in figure 6, which plots MRR under different $n_{neighbor}$ values, HyperEvent framework exhibits distinct patterns that reflect the varying preferences of datasets for long- or short-term historical information. Specifically, on the Wiki dataset, MRR demonstrates remarkable sta-

bility, with values remaining around 80.5 to 81.0 across $n_{neighbor}$ settings. Conversely, the Review dataset shows a pronounced decline, decreasing from 26.8 to 22.0 as $n_{neighbor}$ increases, indicating a sensitivity to shorter history lengths. For the Comment dataset, the change is gradual, with MRR slipping from 75.9 to 75.5. In contrast, the Coin dataset benefits from a longer context, rising steadily from 74.9 to 77.0, while the Flight dataset displays consistent improvement, climbing from 83.3 to 87.7 with higher $n_{neighbor}$.

This divergent behavior originates from the role of $n_{neighbor}$ in defining the temporal scope for constructing hyper-events, as introduced in Section 3.3. Here, $n_{neighbor}$ represents the number of most recent interaction partners stored chronologically in the adjacency table, which directly determines the historical length considered for each node. In HyperEvent, this parameter modulates the input to the correlation-based event association calculations from equations (9) to (16), thereby balancing long-term preferences, such as persistent node affinities over extended timelines, against short-term preferences that focus on immediate, transient interactions. Datasets like Coin and Flight, characterized by slowly evolving patterns, achieve higher MRR with larger $n_{neighbor}$ values, as they leverage richer historical context to accurately identify true hyper-events. In contrast, datasets such as Review and Comment, which involve rapid, high-frequency interactions, perform better with shorter histories, as excessive context may introduce noise that obscures recent relevant events. The findings underscore the adaptability of HyperEvent in capturing dynamic graph dynamics, highlighting how tuning $n_{neighbor}$ effectively addresses the inherent temporal heterogeneities across applications.

Acknowledging space limitations, comprehensive ablation studies investigating the influence of n_{latest} , the contribution of the Enhanced Correlation Vector, and the impact of the Efficient Training Algorithm—are deferred to the supplementary material.

5 Conclusion

Dynamic link prediction in CTDGs faces critical limitations: existing methods neglect intrinsic correlations within composite events and suffer from scalability constraints for large-scale event streams. This paper introduces HyperEvent, a novel framework that fundamentally reframes the prediction task as hyper-event recognition. By defining hyper-events as cohesive sets of correlated temporal events, HyperEvent shifts the paradigm from isolated link prediction to identifying holistic event structures. Our approach employs efficiently computable event correlation vectors to construct interpretable association sequences, explicitly capturing relational patterns between historical events and the query event. Furthermore, we develop a highly scalable parallel training algorithm leveraging precomputed adjacency tables and event stream segmentation, enabling efficient processing of massive graphs. Extensive experiments demonstrate that HyperEvent achieves competitive prediction accuracy while significantly accelerating training throughput.

References

- Ali, A.; Ullah, I.; Ahmad, S.; Wu, Z.; Li, J.; and Bai, X. 2025. An attention-driven spatio-temporal deep hybrid neural networks for traffic flow prediction in transportation systems. *IEEE Transactions on Intelligent Transportation Systems*.
- Chen, J.; Wang, Y.; Zhao, S.; Zhou, P.; and Zhang, Y. 2025. Contextualized Quaternion Embedding Towards Polysemy in Knowledge Graph for Link Prediction. *ACM Transactions on Asian and Low-Resource Language Information Processing*.
- Chen, X.; Zhu, Y.; Xu, H.; Liu, M.; Xiong, L.; Zhang, M.; and Song, L. 2021. Efficient dynamic graph representation learning at scale. arXiv:2112.07768.
- Cho, K.; van Merriënboer, B.; Gulcehre, C.; Bougares, F.; Schwenk, H.; and Bengio, Y. 2014. Learning phrase representations using RNN encoder-decoder for statistical machine translation. In *Conference on Empirical Methods in Natural Language Processing (EMNLP 2014)*.
- Cong, W.; Zhang, S.; Kang, J.; Yuan, B.; Wu, H.; Zhou, X.; Tong, H.; and Mahdavi, M. 2023. DO WE REALLY NEED COMPLICATED MODEL ARCHITECTURES FOR TEMPORAL NETWORKS? In *11th International Conference on Learning Representations, ICLR 2023*.
- Daud, N. N.; Ab Hamid, S. H.; Saadoon, M.; Sahran, F.; and Anuar, N. B. 2020. Applications of link prediction in social networks: A review. *Journal of Network and Computer Applications*, 166: 102716.
- Dileo, M.; Zignani, M.; and Gaito, S. 2024. Temporal graph learning for dynamic link prediction with text in online social networks. *Machine Learning*, 113(4): 2207–2226.
- Duan, G.; Lv, H.; Wang, H.; Feng, G.; and Li, X. 2024. Practical cyber attack detection with continuous temporal graph in dynamic network system. *IEEE Transactions on Information Forensics and Security*.
- Goyal, P.; Chhetri, S. R.; and Canedo, A. 2020. dyn-graph2vec: Capturing network dynamics using dynamic graph representation learning. *Knowledge-Based Systems*, 187: 104816.
- Gravina, A.; Lovisotto, G.; Gallicchio, C.; Bacciu, D.; and Grohnfeldt, C. 2024. Long Range Propagation on Continuous-Time Dynamic Graphs. In *International Conference on Machine Learning*, 16206–16225. PMLR.
- Hajiramezanali, E.; Hasanzadeh, A.; Narayanan, K.; Duffield, N.; Zhou, M.; and Qian, X. 2019. Variational graph recurrent neural networks. *Advances in neural information processing systems*, 32.
- Hochreiter, S.; and Schmidhuber, J. 1997. Long short-term memory. *Neural computation*, 9(8): 1735–1780.
- Huang, S.; Poursafaei, F.; Danovitch, J.; Fey, M.; Hu, W.; Rossi, E.; Leskovec, J.; Bronstein, M.; Rabusseau, G.; and Rabbany, R. 2023. Temporal Graph Benchmark for Machine Learning on Temporal Graphs. *Advances in neural information processing systems*.
- Kipf, T. N.; and Welling, M. 2017. Semi-supervised classification with graph convolutional networks. In *International Conference on Learning Representations*.
- Kumar, S.; Zhang, X.; and Leskovec, J. 2019. Predicting Dynamic Embedding Trajectory in Temporal Interaction Networks. In *Proceedings of the 25th ACM SIGKDD international conference on Knowledge discovery and data mining*. ACM.
- Liang, K.; Meng, L.; Liu, M.; Liu, Y.; Tu, W.; Wang, S.; Zhou, S.; Liu, X.; Sun, F.; and He, K. 2024. A Survey of Knowledge Graph Reasoning on Graph Types: Static, Dynamic, and Multi-Modal. *IEEE Transactions on Pattern Analysis and Machine Intelligence*, 46(12): 9456–9478.
- Luo, Y.; and Li, P. 2022. Neighborhood-aware scalable temporal network representation learning. In *Learning on Graphs Conference*, 1–1. PMLR.
- Manessi, F.; Rozza, A.; and Manzo, M. 2020. Dynamic graph convolutional networks. *Pattern Recognition*, 97: 107000.
- Min, S.; Gao, Z.; Peng, J.; Wang, L.; Qin, K.; and Fang, B. 2021. Stgsn—a spatial-temporal graph neural network framework for time-evolving social networks. *Knowledge-Based Systems*, 214: 106746.
- Ong, R.; Sun, J.; Guo, Y.-K.; and Serban, O. 2025. Dynamic link prediction: Using language models and graph structures for temporal knowledge graph completion with emerging entities and relations. *Expert Systems with Applications*, 126648.
- Pareja, A.; Domeniconi, G.; Chen, J.; Ma, T.; Suzumura, T.; Kanezashi, H.; Kaler, T.; Schardl, T.; and Leiserson, C. 2020. Evolvegc: Evolving graph convolutional networks for dynamic graphs. In *Proceedings of the AAAI conference on artificial intelligence*, volume 34, 5363–5370.
- Poursafaei, F.; Huang, S.; Pelrine, K.; and Rabbany, R. 2022. Towards better evaluation for dynamic link prediction. *Advances in Neural Information Processing Systems*, 35: 32928–32941.
- Qin, Y.; Ju, W.; Wu, H.; Luo, X.; and Zhang, M. 2024. Learning Graph ODE for Continuous-Time Sequential Recommendation. *IEEE Transactions on Knowledge and Data Engineering*, 36(7): 3224–3236.
- Rakshit Trivedi, P. B., Mehrdad Farajtabar; and Zha, H. 2019. Dyrep: Learning representations over dynamic graphs. In *7th International Conference on Learning Representations (ICLR)*.
- Rossi, E.; Chamberlain, B.; Frasca, F.; Eynard, D.; Monti, F.; and Bronstein, M. 2020. Temporal Graph Networks for Deep Learning on Dynamic Graphs. arXiv:2006.10637.
- Scarselli, F.; Gori, M.; Tsoi, A. C.; Hagenbuchner, M.; and Monfardini, G. 2008. The graph neural network model. *IEEE transactions on neural networks*, 20(1): 61–80.
- Vaswani, A.; Shazeer, N.; Parmar, N.; Uszkoreit, J.; Jones, L.; Gomez, A. N.; Kaiser, Ł.; and Polosukhin, I. 2017. Attention is all you need. *Advances in neural information processing systems*, 30.
- Wang, L.; Chang, X.; Li, S.; Chu, Y.; Li, H.; Zhang, W.; He, X.; Song, L.; Zhou, J.; and Yang, H. 2021a. TCL: Transformer-based Dynamic Graph Modelling via Contrastive Learning. arXiv:2105.07944.

Wang, Y.; Chang, Y.-Y.; Liu, Y.; Leskovec, J.; and Li, P. 2021b. Inductive Representation Learning in Temporal Networks via Causal Anonymous Walks. In *International Conference on Learning Representations (ICLR)*.

Xu, D.; Ruan, C.; Korpeoglu, E.; Kumar, S.; and Achan, K. 2020. Inductive Representation Learning on Temporal Graphs. In *8th International Conference on Learning Representations, ICLR 2020*.

Xu, Y.; Zhang, W.; Xu, X.; Li, B.; and Zhang, Y. 2025. Scalable and Effective Temporal Graph Representation Learning With Hyperbolic Geometry. *IEEE Transactions on Neural Networks and Learning Systems*, 36(4): 6080–6094.

Yan, X.; Weiha, W.; and Chang, M. 2021. Research on financial assets transaction prediction model based on LSTM neural network. *Neural Computing and Applications*, 33(1): 257–270.

Yang, X.; Zhao, X.; and Shen, Z. 2025. A generalizable anomaly detection method in dynamic graphs. In *Proceedings of the AAAI Conference on Artificial Intelligence*, volume 39, 22001–22009.

Yu, L.; Sun, L.; Du, B.; and Lv, W. 2023. Towards better dynamic graph learning: New architecture and unified library. *Advances in Neural Information Processing Systems*, 36: 67686–67700.

Zhang, M.; Wu, S.; Yu, X.; Liu, Q.; and Wang, L. 2023. Dynamic Graph Neural Networks for Sequential Recommendation. *IEEE Transactions on Knowledge and Data Engineering*, 35(5): 4741–4753.

Zhang, X.; Wang, Y.; Wang, X.; and Zhang, M. 2024. Efficient Neural Common Neighbor for Temporal Graph Link Prediction. arXiv:2406.07926.

Zou, G.; Lai, Z.; Wang, T.; Liu, Z.; and Li, Y. 2024. Mt-stnet: A novel multi-task spatiotemporal network for highway traffic flow prediction. *IEEE Transactions on Intelligent Transportation Systems*.

A Complexity Analysis

This section provides a detailed analysis of the computational efficiency of the HyperEvent framework, examining both time and space complexity characteristics. The analysis reveals significant advantages over existing temporal graph learning approaches, particularly in enabling large-scale processing.

Time Complexity per query event prediction is decomposed as follows: *i) Adjacency Table Maintenance*: Requires $\mathcal{O}(1)$ operations per event insertion due to fixed-length neighbor storage, enabling real-time updates. *ii) Hyper-event Extraction*: Achieves $\mathcal{O}(1)$ lookup by directly accessing precomputed neighbor lists in \mathcal{A} , eliminating neighborhood sampling costs. *iii) Relational Vector Calculation*: Consumes $\mathcal{O}(n_{\text{neighbor}}^2)$ operations per event due to pairwise neighbor comparisons, but remains independent of overall graph size. With constrained n_{neighbor} and optimized 2-hop calculation using $\lfloor \sqrt{n_{\text{neighbor}}} \rfloor$ neighbors, this reduces to practical constant time. *iv) Discriminator Inference*: Transformer processing exhibits $\mathcal{O}((n_{\text{latest}})^2 \cdot d_{\text{model}})$ complexity per hyper-event, where n_{latest} is small and the number of model channels d_{model} is fixed.

The aggregate $\mathcal{O}(1)$ neighborhood operations demonstrate independence from global graph scale $|\mathcal{V}|$ or $|\mathcal{E}|$, enabling constant-time prediction scaling.

Space Complexity is dominated by: *i) Adjacency Tables*: Require $\mathcal{O}(|\mathcal{V}| \cdot n_{\text{neighbor}})$ storage, linear in node count but with small constant n_{neighbor} (typically ≤ 50). *ii) Segment Precomputation*: Efficient training adds $\mathcal{O}(n_{\text{segment}} \cdot |\mathcal{V}| \cdot n_{\text{neighbor}})$ storage for boundary adjacency tables, trading marginal space overhead for massive parallelism. *iii) Discriminator Parameters*: Occupy fixed $\mathcal{O}(d_{\text{model}}^2)$ space independent of graph dynamics.

The $\mathcal{O}(|\mathcal{V}|)$ spatial scaling is substantially efficient, particularly given the multiplicative constant n_{neighbor} is empirically shown to be small. When combined with the segment-level parallelism, HyperEvent achieves unprecedented scalability: The framework efficiently processes temporal graphs of tens of millions of edges through parallel training, while maintaining constant-time prediction latency for individual queries, overcoming critical bottlenecks in streaming graph learning.

B Experimental Setup

B.1 Datasets

HyperEvent is evaluated using the Temporal Graph Benchmark (TGB), a comprehensive repository containing five temporal graph datasets for dynamic link prediction. Following TGB’s standardized protocol, all datasets are chronologically partitioned into training (70%), validation (15%), and test sets (15%) to ensure temporally meaningful evaluation. The experiments span five large-scale datasets representing diverse real-world dynamics: **1) Wiki** (tgbl-wiki-v2): Captures bipartite user-page interactions from Wikipedia co-editing logs, featuring text-attributed edges. **2) Review** (tgbl-review-v2): Contains weighted user-product interactions from Amazon electronics reviews (1997–2018). **3)**

Dataset	Domain	Nodes	Edges	Steps	Surprise	Edge Properties
tgbl-wiki	interact	9,227	157,474	152,757	0.108	W: ×, Di: ✓, A: ✓
tgbl-review	rating	352,637	4,873,540	6,865	0.987	W: ✓, Di: ✓, A: ×
tgbl-coin	transact	638,486	22,809,486	1,295,720	0.120	W: ✓, Di: ✓, A: ×
tgbl-comment	social	994,790	44,314,507	30,998,030	0.823	W: ✓, Di: ✓, A: ✓
tgbl-flight	traffic	18,143	67,169,570	1,385	0.024	W: ×, Di: ✓, A: ✓

Table 3: TGB dataset statistics

Coin (tgbl-coin-v2): Documents cryptocurrency transactions during the 2022 Terra Luna market crash. **4) Comment** (tgbl-comment): Models directed reply networks from Reddit (2005–2010), comprising over 44 million edges. **5) Flight** (tgbl-flight-v2): Represents global airport traffic (2019–2022) with geo-attributed nodes and flight-number edges.

As detailed in Table 3, these graphs exhibit substantial heterogeneity in scale (638K–18M nodes, 157K–67M edges), temporal dynamics (1,385–30M timestamps), and edge characteristics (weighted, directed, and attributed). The dynamic link prediction task consistently requires forecasting the next event given historical event streams.

All experiments implement the standardized evaluation protocols from TGB. This includes chronological train/validation/test splits and standardized negative queries for dynamic link prediction. While several datasets include node features or edge attributes/weights, such information is deliberately excluded. This choice isolates and highlights HyperEvent’s capacity to capture intrinsic event interdependencies, demonstrating the framework’s efficacy without relying on external features.

B.2 Evaluation Metric

The filtered Mean Reciprocal Rank (MRR) as specified by TGB is adopted, representing a ranking-based metric particularly suited for dynamic link prediction. Unlike Area Under the ROC Curve or Average Precision, which fail to adequately capture the relative ranking of positive edges against negatives, MRR directly measures the reciprocal rank of the true destination node among negative candidates. This aligns with recommendation systems and knowledge graph completion tasks where ranking quality is paramount. Crucially, all negative edges are predefined in TGB benchmark, ensuring fair comparison across methods.

Formally, for each positive query edge with prediction score y_{pos} , and a set of negative candidate scores y_{neg} , HyperEvent computes *Optimistic rank*: Number of negatives scoring strictly higher than y_{pos} . *Pessimistic rank*: Number of negatives scoring at least y_{pos} . The final rank r is averaged:

$$r = \frac{1}{2}(\text{optimistic_rank} + \text{pessimistic_rank}) + 1. \quad (19)$$

MRR is then calculated as:

$$\text{MRR} = \frac{1}{|Q|} \sum_{i=1}^{|Q|} \frac{1}{r_i}, \quad (20)$$

Parameter	Dataset				
	Wiki	Review	Coin	Comment	Flight
n_{neighbor}	15	10	40	10	50
n_{latest}	10	10	10	10	10
n_{segment} in Train	50	50	50	20	50
n_{segment} in Val/Test	1	10	20	10	20

Table 4: HyperEvent parameter configurations on different datasets

where Q is the set of test queries. MRR ranges within (0,1], with higher values indicating superior ranking performance. This metric reflects the growing consensus in recent graph representation learning literature for assessing link prediction quality.

B.3 HyperEvent Parameters

HyperEvent employs three key hyperparameters: n_{neighbor} , n_{latest} , and n_{segment} . The hyperparameter n_{segment} primarily governs computational efficiency by segmenting the event stream for parallel processing. Selection of n_{segment} balances GPU memory constraints with training duration relative to dataset scale. During evaluation, which involves processing multiple negative samples concurrently, a smaller n_{segment} value is typically used compared to training. For the Wiki, Review, and Comment datasets, the optimal n_{neighbor} was searched within {10, 15, 20}, with n_{latest} fixed at 10. Observations indicated a preference for larger neighborhoods on Coin and Flight datasets, prompting a search over {10, 15, 20, 30, 40, 50} for n_{neighbor} . The hyperparameter n_{latest} was optimized from {5, 8, 10} when fixing $n_{\text{neighbor}} = 10$. Detailed hyperparameter configurations for all datasets are provided in Table 4.

B.4 Transformer Architecture

The hyper-event discriminator utilizes a Transformer module. As this component does not represent a core innovation, a fixed architectural configuration was employed across all datasets without dataset-specific tuning. The settings include: a maximum sequence length of 512 for position encoding, position encoding dimension of 64, Transformer hidden dimension of 64, 3 layers, 4 attention heads, dropout rate of 0.1, and GELU activation functions.

B.5 Training Protocol

Optimization employed Adam with a fixed learning rate of 0.0001. The model was trained for 50 epochs on the Wiki

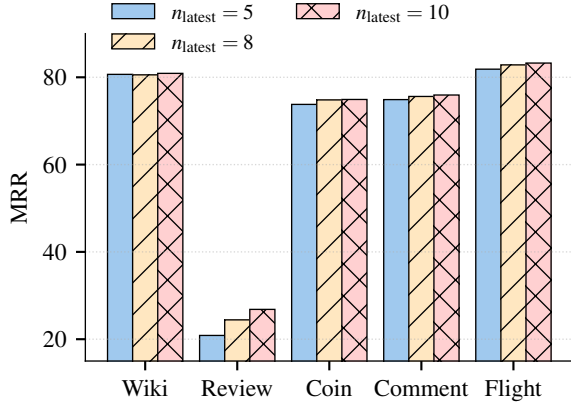


Figure 7: MRR across different datasets under varying n_{latest} (fix $n_{\text{neighbor}} = 10$).

dataset and 5 epochs on all other datasets. Model selection was based on performance on the validation set, with final results reported on the test set using the MRR metric. The mean and standard deviation of MRR over 5 independent runs with different random seeds are reported to ensure statistical reliability.

B.6 Hardware

All experiments were conducted on a high-performance computing system equipped with an Intel Core i7-14700KF CPU, 64 GB RAM, and an NVIDIA GeForce RTX 4090 GPU with 24 GB VRAM.

B.7 Ablation Study

Influence of n_{latest} Figure 7 evaluates MRR under varying values of n_{latest} (5, 8, and 10). The figure illustrates that MRR exhibits minimal variation across these settings for most datasets. Specifically, on Wiki, Coin, Comment, and Flight, the MRR values remain stable with only slight fluctuations as n_{latest} increases, indicating limited sensitivity to this parameter. The sole exception is the Review dataset, where MRR shows notable differences—rising from the baseline at $n_{\text{latest}} = 5$ to higher values at $n_{\text{latest}} = 10$.

This behavior can be attributed to the definition of n_{latest} , which directly governs the number of recent events aggregated into a hyper-event. Datasets primarily rely on n_{neighbor} to encode long- and short-term historical preferences; n_{neighbor} effectively captures node-level temporal dependencies, thereby reducing the influence of n_{latest} on overall predictive performance. Furthermore, excessively increasing n_{latest} escalates computational overhead due to the linear scaling of event aggregation in hyper-event formation, without delivering commensurate gains in accuracy for most scenarios. Consequently, adopting $n_{\text{latest}} = 10$ strikes an optimal balance, providing robust predictive capabilities while maintaining computational efficiency across diverse dynamic graph environments.

Dataset	Enhanced Correlation Vector		Drop
	with	without	
Wiki	80.90	77.62	4.06%
Review	26.83	8.61	67.91%
Coin	74.92	66.23	11.60%
Comment	75.94	53.83	29.12%
Flight	83.26	74.27	10.80%

Table 5: MRR of HyperEvent with/without Enhanced Correlation Vector

Without the Enhanced Correlation Vector This ablation evaluates the Enhanced Correlation Vector’s contribution by comparing model performance when replacing the full 12-dimensional correlation vector with a reduced version using only 1-hop neighborhood overlap distance. As Table 5 indicates, removing multi-hop structural correlations causes consistent and substantial performance degradation. The MRR drops range from 4.06% on Wiki to a drastic 67.91% on Review, with all five datasets exhibiting declines exceeding 10% except Wiki. This degradation proves particularly severe for datasets like Review and Comment, where node interactions involve complex higher-order dependencies.

Two key factors explain this sensitivity. First, limiting correlation modeling to immediate (1-hop) neighborhoods overlooks critical structural contexts captured by 0-hop (node identity correlation) and 2-hop (extended topology correlation) features. For example, on Review, where users interact sequentially across diverse products, 0-hop identity matching helps confirm recurring user/item relationships, while 2-hop signals reveal indirect influence chains. Second, the impoverished 4-dimensional vector lacks granularity to discriminate between genuine hyper-events and coincidental event aggregations. Consequently, the model frequently misclassifies valid query events that rely on multi-scale evidence, especially for inductive cases involving unseen nodes where 1-hop patterns alone are insufficient to confirm hyper-event integrity. These results validate that comprehensive correlation modeling—spanning local to global neighborhood contexts—is indispensable for robust hyper-event recognition.

Without the Efficient Training Algorithm Table 6 quantitatively compares per-epoch training durations for HyperEvent with and without the proposed efficient training algorithm across five temporal graph datasets. A striking observation emerges: enabling this algorithm consistently reduces training times by over 95% across all datasets, achieving relative savings exceeding 98% on four benchmarks. Notably, the degree of acceleration correlates with the segmentation parameter n_{segment} . Higher n_{segment} values yield more significant efficiency gains, as evidenced by the 98.07% saving on Flight ($n_{\text{segment}} = 50$) versus 95.03% on Comment ($n_{\text{segment}} = 20$).

This dramatic improvement stems from the algorithm’s core design: partitioning the monolithic event stream into n_{segment} independent segments linearly reduces the effective

Dataset	Efficient Training Algorithm		Time Saved Relative
	with	without	
Wiki	9s ($n_{\text{segment}} = 50$)	7m 44s	98.08%
Review	4m 43s ($n_{\text{segment}} = 50$)	4h 02m 19s	98.06%
Coin	22m 05s ($n_{\text{segment}} = 50$)	18h 49m 02s	98.04%
Comment	1h 47m 48s ($n_{\text{segment}} = 20$)	35h 47m 28s	95.03%
Flight	1h 04m 45s ($n_{\text{segment}} = 50$)	55h 49m 05s	98.07%

Table 6: Per-epoch Training Time of HyperEvent with/without Efficient Training Algorithm

event sequence length processed within each iteration from $|\mathcal{E}|$ to $\frac{|\mathcal{E}|}{n_{\text{segment}}}$. Simultaneously, tensorized implementation can fully leverage the massive parallel computing capabilities of GPUs while avoiding multithreading overhead. Consequently, the computational complexity per epoch scales inversely with n_{segment} , explaining the near-linear time reduction observed. Such efficiency is imperative for scaling HyperEvent to massive real-world temporal graphs, where raw training times without segmentation proved prohibitive (e.g., exceeding 55 hours per epoch on Flight). This approach transforms HyperEvent from a conceptual framework into a practically deployable solution for industrial-scale dynamic graphs.